

# Experimental Study of Diffraction by a Thin Cone

Belous A.A., Korolkov A.I., Shanin A.V.

Faculty of Physics, Lomonosov Moscow State University, Russia; e-mail: artem.belous@gmail.com

A problem of diffraction of acoustical waves by a thin rigid cone is studied. A direct diffraction experiment is used to measure the diffracted field on the surface of a thin cone. The experiment is performed using MLS (Maximum Length Sequence) method. The cases of axial and non-axial incidence are studied. The wavelengths are small compared to the cone size. Boundary integral equation method is used to describe the field theoretically in parabolic approximation. The integral equation is solved numerically by iterations. The results of the experiment are compared with the results of the calculation.

## 1 INTRODUCTION

Diffraction by a thin cone attracts considerable attention of researchers. Several different approaches exist to developing both asymptotics of the diffracted field and the diffracted field itself. First, there is a traditional asymptotic approach based on ray representation [1]. Second, there is an approach based on the parabolic equation method [2]. Third, there is an approach based on boundary integral equation method for the parabolic equation in Cartesian coordinates [3]. Also, there is an approach based on the Smyshlyaev's formula [4], and another one based on Kontorovich-Lebedev integral representation [5]. Still, authors know no works devoted to experimental study of this problem. In this work we are trying to fill this gap.

A direct diffraction experiment is used to measure the diffracted field on the surface of a cone. The experiment is performed using MLS technique [6]. The receiver is put on the surface of the cone. After that the cone is irradiated by a point source from different directions so that the receiver is enlightened or shadowed. Boundary integral equation method in parabolic approximation [7] is used to validate the results of the experiment.

## 2 EXPERIMENT

### 2.1 Description

A narrow (the vertex angle is  $2\alpha = 5.5^\circ$ ) 1 meter long duralumin cone (see Fig. 1) is hanged in free space. A small (the size is around 0.01 meter) microphone is placed on the surface of the cone. The

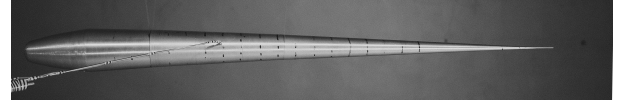


Figure 1: Photo of the duralumin cone with the microphone on its surface.

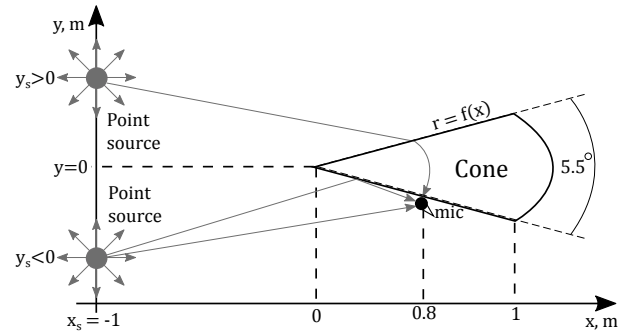


Figure 2: Experiment scheme, view from above.

cone is irradiated by a small sound source (its size is around 0.01 meter) from different directions so the microphone can be shadowed or enlightened (see Fig. 2). A miniature Knowles RAB-32257 armature driver is used as a source and a well-calibrated no-name microphone is used as a receiver.

To conduct the experiment, MLS method is used [6]. The cone is irradiated with a pseudo-random signal and then impulse response of the acoustical path is calculated via calculating correlation of the MLS signal with the output signal.

The input MLS signal is correlated with the measured signal (see Fig. 3) and impulse response is calculated. A region of interest corresponding to diffraction by the cone is cropped from impulse response. After that a frequency image of the impulse response is calculated and compared to theory.

## 3 THEORETICAL DESCRIPTION

### 3.1 Problem statement

Let us consider a stationary 3D problem and omit the time-dependence  $\exp\{-i\omega t\}$ . The acoustical field satisfies Helmholtz equation everywhere out-

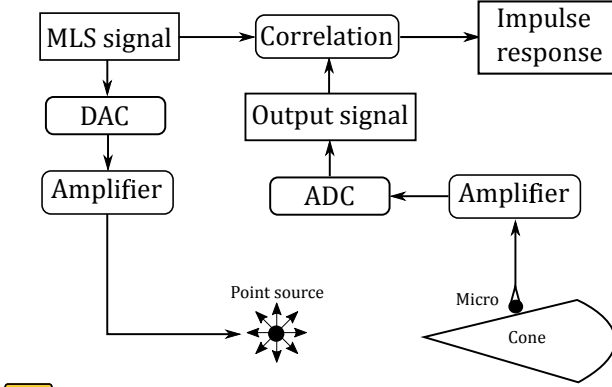


**Figure 3:** Experimental data processing scheme.

side the cone:

$$\Delta \tilde{u} + k^2 \tilde{u} = 0, \quad (1)$$

where  $\Delta$  is the Laplace operator. The cone is rigid, so the full field satisfies the Neumann boundary conditions:

$$\frac{\partial \tilde{u}}{\partial \vec{n}} = 0, \quad (2)$$

where  $\vec{n}$  is the normal vector to the cone surface. The cone is very narrow (the vertex angle is much smaller than 1 radian) so most of the waves are supposed to be scattered under small angles. This means that the parabolic approximation can be used to describe the diffraction processes [7]. Following the standard procedure the field is represented in the following form:

$$\tilde{u}(x, r, \varphi) = \exp \{ikx\} u(x, r, \varphi), \quad (3)$$

where  $u$  is a slow function of  $x$ , compared to the exponential factor. Substituting (3) in (1) and neglecting the small terms, get the approximate equation for  $u$ :

$$\left( \frac{\partial}{\partial x} + \frac{1}{2ik} \Delta_{\perp} \right) u = 0, \quad (4)$$

where

$$\Delta_{\perp} = \left( \frac{1}{r} \frac{\partial}{\partial r} r \frac{\partial}{\partial r} + \frac{1}{r^2} \frac{\partial^2}{\partial \varphi^2} \right). \quad (5)$$

This is the parabolic equation of the diffraction theory.

The field  $u$  is represented as a sum of the incident and the scattered field:

$$u = u^{\text{in}} + u^{\text{sc}}. \quad (6)$$

As we are using a point source in the experiment,  $u^{\text{in}}$  is equal to Green's function of the parabolic equation. Let us denote the points of space by  $\vec{r} = (x, r, \varphi)$  and the point source be located at  $\vec{r}_s = (x_s, r_s, \varphi_s)$ . Hence

$$u^{\text{in}} = \frac{k}{2\pi i(x - x_s)} \exp \left[ \frac{ik}{2} \frac{(\Delta r)^2}{x - x_s} \right], \quad x > x_s. \quad (7)$$

where  $\Delta r$  is the distance between the projections of  $\vec{r}$  and  $\vec{r}_s$  onto the transversal plane:

$$(\Delta r)^2 = r^2 + r_s^2 - 2rr_s \cos(\varphi - \varphi_s). \quad (8)$$

Note that  $u^{\text{in}}$  is equal to zero if  $x < x_s$ .

The problem statement should be supplemented with radiation and Meixner conditions. For details see [7].

### 3.2 Calculating the diffracted field

In [7] a boundary integral equation is derived for the field diffracted by a body of revolution. The equation is applied to the bodies having their radii dependent on  $x$  like  $r = f(x)$ . Here the authors are going to apply the results of [7] to the cone problem.

Let  $U(x, \varphi)$  be the full field on the surface,  $U^{\text{in}}$  be the incident field on the surface, i.e.

$$U^{\text{in}}(x, \varphi) \equiv u^{\text{in}}(x, f(x), \varphi), \quad (9)$$


$$U(x, \varphi) \equiv u(x, f(x), \varphi). \quad (10)$$

Denote  $x_*, \varphi_*$  as the observation point coordinates on the cone surface. Then the following integral equation is satisfied:

$$U(x_*, \varphi_*) = \int_0^{2\pi} \int_0^{x_*} K(x_*, \varphi_*, x, \varphi) U(x, \varphi) dx d\varphi + 2U^{\text{in}}(x_*, \varphi_*), \quad (11)$$

$$K(x_*, \varphi_*, x, \varphi) = \frac{ikf(x)}{2\pi} \times \left[ \frac{\dot{f}(x)}{x_* - x} + \frac{f(x) - f(x_*) \cos(\varphi - \varphi_*)}{(x_* - x)^2} \right] \times \exp \left\{ \frac{ik}{2} \frac{f^2(x_*) + f^2(x) - 2f(x_*)f(x) \cos(\varphi - \varphi_*)}{x_* - x} \right\}, \quad (12)$$

For our case  $f(x)$  is a linear function of  $x$ ,  $r = f(x) = x \tan \alpha \approx x\alpha$ , where  $2\alpha$  is the angle at the vertex of our cone.

Note that equation (11) is of Volterra type  with respect to variable  $x$ , and is of difference kernel type with respect to variable  $\varphi$ . This means that it can be solved using iterations with respect to  $x$ .

Let us solve the equation numerically using the method of approximation with linear basis functions [8]. The following basis functions  $N_i(x)$  are used:

$$N_i(x) = \begin{cases} 0, & x_{i-1} > x \\ (x - x_{i-1})/(x_i - x_{i-1}), & x_i > x > x_{i-1} \\ (x_{i+1} - x)/(x_{i+1} - x_i), & x_{i+1} > x > x_i \\ 0, & x > x_{i+1}, \end{cases} \quad (13)$$

i. e.  $N_i(x)$  is a triangle basis function. The solution  $U$  is sought in the form:

$$U(x, \varphi) \approx \sum_{i=1}^M U_i(\varphi) N_i(x), \quad (14)$$

where  $U_i(\varphi)$  are some unknown functions. We substitute (14) in (11) and get the following system of linear integral equations:


$$U_i(\varphi_*) = \sum_{j=1}^M \int_0^{2\pi} K_{ij}(\varphi_*, \varphi) U_j(\varphi) d\varphi + 2U_i^{\text{in}}(\varphi_*), \quad i = 1 \dots M, \quad (15)$$

where

$$U_i^{\text{in}}(\varphi_*) \equiv U^{\text{in}}(x_i, \varphi_*), \quad (16)$$

$$K_{ij}(\varphi_*, \varphi) \equiv \int_0^{x_i} K(x_i, \varphi_*, x, \varphi) N_j(x) dx, \quad (17)$$

One can notice that the integrand in (17) oscillates near the point  $x = x_i$  which can possibly be a source of numerical errors. To solve this issue the contour of integration should be slightly shifted to the upper complex half-plane where the kernel  $K$  decays exponentially.

Then, the system (15) is discretized using finite difference method  and solved with iterations for each frequency.

## 4 EXPERIMENTAL RESULTS AND MODELING

### 4.1 Axial incidence

In the case of axial incidence ( $y_s = 0$ ) there was almost no diffraction observed, i. e. the field measured on the surface of the cone was close to the free

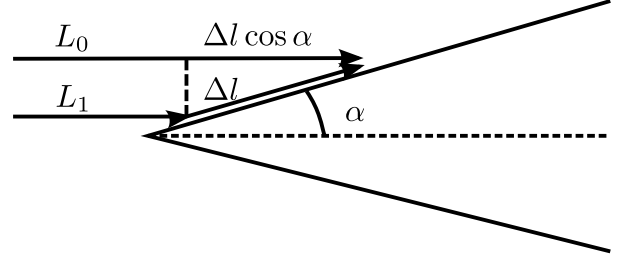



Figure 4: Illustration to calculation of the Fresnel zone size (18)

field of the point source. This result may look a little surprising, but let us explain it in terms of Fresnel zone approach. It is supposed that diffraction on an obstacle occurs when the obstacle is covered by several Fresnel zones. Let us note that in our experiment we use the frequencies in range 2000 - 10000 Hz. In this range we can approximately suppose that the cone is irradiated by plane waves, since the source was 1 meter far from the cone's vertex. The difference of path lengths between the shortest ray and the ray diffracted by the cone can then be easily estimated (see Fig. 4): 

$$L_1 - L_0 = \Delta l(1 - \cos \alpha) \approx \Delta l \alpha^2 / 2, \quad (18)$$

The first Fresnel zone size  $\Delta l$  is determined by equating the latter to  $\lambda/2$ :

$$\Delta l = \lambda / \alpha^2. \quad (19)$$

Thus, for the highest frequency the size of the first Fresnel zone  $\Delta l$  is around 15 meters which is 15 times bigger than the total length of the cone. That is why we see no diffraction in the case of axial incidence. We should note that the same result is provided by the solution of equation (15).

### 4.2 Non-axial incidence

Using a calculation similar to (18) one can show that diffraction process becomes more noticeable when the source is shifted towards the axis perpendicular to that of the cone. The experiment confirms this reasoning. The results of the experiment for shifts  $y_s = \pm 0.5, \pm 0.3, \pm 0.1$  meters and  $x_s = -1$  m compared with the respective results of the solution of equation (15) is shown in Fig. 5, Fig. 6, Fig. 7 correspondingly. The receiver was put near the surface of the cone with its  $x$ -coordinate equal to 0.8 m, as shown in Fig. 2. We present

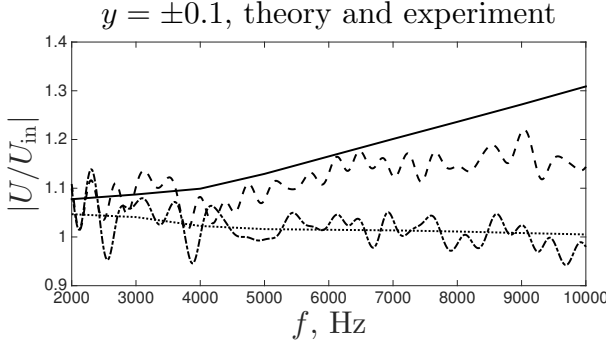


Figure 5: Comparison of experiment and theory for  $y = \pm 0.1$  m. Theory (solid line) and experiment (dashed line) for  $y = -0.1$  m, theory (dotted line) and experiment (dash-dotted line) for  $y = 0.1$  m.

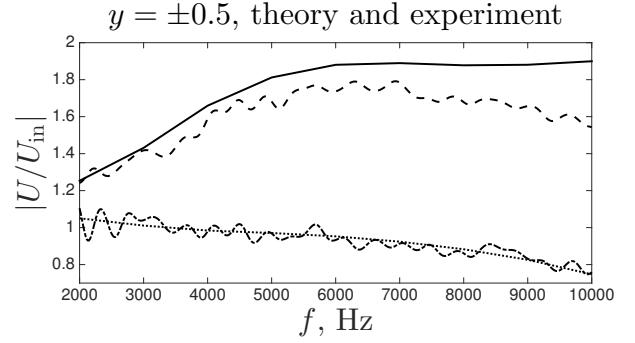


Figure 7: Comparison of experiment and theory for  $y = \pm 0.5$  m. Theory (solid line) and experiment (dashed line) for  $y = -0.5$  m, theory (dotted line) and experiment (dash-dotted line) for  $y = 0.5$  m.

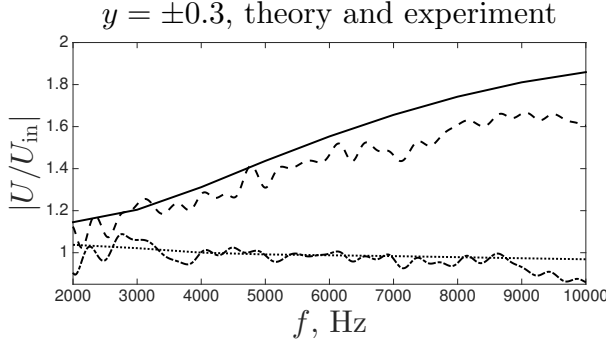


Figure 6: Comparison of experiment and theory for  $y = \pm 0.3$  m. Theory (solid line) and experiment (dashed line) for  $y = -0.3$  m, theory (dotted line) and experiment (dash-dotted line) for  $y = 0.3$  m.

the absolute values  $|U/U_{in}|$  to exclude the geometrical attenuation of the field. In other words, value  $U/U_{in}$  can be considered as an approximation to the field of the plane wave diffraction problem.

The following natural conclusions can be made from the experiment. First, the absolute value of the field in the enlightened zone ( $y_s < 0$ ) is bigger than in the shadow ( $y_s > 0$ ). Second, the value  $|U/U_{in}|$  in the enlightened zone tends to 2 as frequency grows which corresponds to the case of reflection from hard wall, and tends to 0 in shadow.

The authors associate the theory-experiment discrepancies with positioning errors, electrical noises in the equipment, and imperfections of the source and microphone. Also let us note that accuracy of the parabolic approximation decreases as  $|y_s|$

grows, since the diffraction process cannot be considered paraxial. In the upcoming papers the authors are going to pay more attention to these problems and to provide comparisons with some other existing theoretical approaches [1, 2, 4, 5].

## 5 CONCLUSION

In this work, a direct acoustical diffraction experiment has been held on diffraction by a narrow rigid cone with the use of a point source and MLS technique. The results of the experiment for axial incidence show that there is almost no diffraction due to a big longitudinal size of the Fresnel zone along the cone surface. For non-axial incidence (if the angle of incidence is small enough) the results agree with the solution of boundary integral equation in parabolic approximation.

## ACKNOWLEDGEMENTS

The work is supported by the RSF grant 14-22-00042.

## REFERENCES

- [1] Popov A., Ladyzhensky A., Khozioski S., 2009, Uniform Asymptotics of the Wave Diffracted by a Cone of Arbitrary Cross Section, *Russ. J. Math. Phys.*. Vol. 16, no. 2, p. 296-299.
- [2] Andronov I. V., 2011, Diffraction by a Strongly Elongated Body of Revolution, *Acoust. Phys.*. Vol. 57, p. 147-152.

- [3] A.V Shanin, A.I Korolkov, 2017, Diffraction by a thin cone in the parabolic approximation. Method of the boundary integral equation, *ICEAA Proceedings 2017*, DOI: 10.1109/ICEAA.2017.8065342
- [4] V.M Babich, D.B Dement'ev, B.A Samokish, V.P Smychlyayev, 2000, On evaluation of the diffraction coefficient for arbitrary "nonsingular" directions of a smooth convex cone, *SIAM J. Appl. Math.*, Vol. **60**, no. **2**, p. 536–573.
- [5] Lyalinov M. A., Zhu N. Y., 2007, Acoustic scattering by a circular semitransparent conical surface, *J. Eng. Math.*, Vol. **59**, no. **4**, p. 385–398.
- [6] Shanin A. V., Valyaev V. Yu., 2011, Maximum length sequence method in diffraction experiment, *Acoustical Physics*. Vol **57**, no. **3**, p. 420–425.
- [7] Shanin A. V., Korolkov A.I., 2018, Diffraction by an elongated body of revolution. A boundary integral equation based on the parabolic equation, *arxiv.org* arXiv:1704.08857v1.
- [8] Zienkiewicz O. C., Taylor R. L. The Finite element method Volume 1: The Basis, Oxford, Butterworth-Heinemann, 2000.